Turk J Pharm Sci 2023;20(1):23-34
DOI: 10.4274/tjps.galenos.2022.93275

ORIGINAL ARTICLE

Resveratrol-Loaded Microsponge Gel for Wound Healing: *In Vitro* and *In Vivo* Characterization

Vinita Chandrakant PATOLE[1]*, Devyani AWARI[2], Shilpa CHAUDHARI[3]

[1]Dr. D.Y. Patil Institue of Pharmaceutical Sciences and Research, Department of Pharmaceutics, Pune, India
[2]Datta Meghe Institute of Medical Sciences (Deemed to be University), Datta Meghe College of Pharmacy, Maharashtra, India
[3]Dr. D.Y. Patil College of Pharmacy, Department of Pharmaceutics, Pune, India

ABSTRACT

Objectives: The study was aimed to formulate resveratrol (RSV) loaded microsponges to deliver drug at the wound site and incorporate it in the *Moringa oleifera* Lam. (Moringaceae) gel base to provide an appropriate moist environment for wound management. RSV, a stilbenoid that activates sirtuins and cell-signaling regulators involved in the process of wound healing.

Materials and Methods: Microsponges were prepared by oil in oil emulsion solvent diffusion method by optimizing the independent variables; drug: polymer ratio and volume of internal phase solvent and their effects on entrapment efficiency and particle size. Formulation batches were evaluated for drug content, production yield, entrapment efficiency, and *in vitro* drug release. The microsponges were further incorporated into *M. oleifera* gum gel, which was then evaluated for spreadability, viscosity, *ex vivo* diffusion study and *in vivo* studies using an excision wound model in rats.

Results: Scanning electron microscopy revealed spherical and porous nature of the microsponges *in vitro*-release study of the optimized batch of RSV microsponges showed 80.88% drug release within 8 h. Differential scanning calorimetry results revealed no drug and polymer interaction during the formation of microsponges. An *ex vivo* diffusion study through goat skin revealed sustained release of RSV through porous microsponges embedded in the gel base at the wound site. An *in vivo* study performed using an excision wound model showed wound healing and closure within day 8. Histopathology showed increased re-epithelization and reduced ulceration in RSV microsponge gel-treated group compared with sham operated.

Conclusion: RSV microsponge gel delivered the drug at the wound site and the gel base provided a moist environment and influenced cell adhesion, thereby promoting faster wound healing.

Key words: Resveratrol, microsponges, wound healing, *Moringa oleifera* gum, excision wound model

INTRODUCTION

Microsponges are polymeric drug delivery systems composed of porous structure.[1,2] These are tiny porous, sponge-like spherical particles with a surface area of 5 to 150 mm. The major advantages of microsponges are good entrapment efficiency with good stability at high pH and temperature. Due to their porous structure, they can extend the drug release.[3] Emulsion solvent diffusion, suspension polymerization, or oil in oil emulsion solvent diffusion methods are used for the formulation of microsponges.[4] Microsponges encapsulate the drug and this technique of microencapsulation helps control drug release rates and prolong the release time.[5]

To formulate microsponges, one of the preferred polymers is Eudragit RL 100 to control the drug release of the formulation. Eudragit RL 100 is methacrylic acid esters possessing hydrophilic properties due to the presence of more amounts of quaternary ammonium groups compared to Eudragit RS 100. This nature of Eudragit RL 100 helps improve the water uptake capacity, which is required for the rapid absorption of exudates from wound, maintaining its ability to preserve water required for wound healing.[6] The cationic nature of Eudragit RL helps it interact strongly with the negatively charged mucins *via* electrostatic attraction, increasing its bio-adhesivity.[7] Also, Eudragit RL 100 is reported to permit water vapor and oxygen permeation, which is required for wound healing.[8]

Resveratrol (RSV) (3,5,40-trihydroxy-*trans*-stilbene), a natural polyphenolic compound present in grape skin, peanuts, and red wine.[9,10] It belongs to Biopharmaceutical Classification System

*Correspondence: vinitapawara@gmail.com, Phone: +9730388345, ORCID-ID: orcid.org/0000-0001-9544-4074
Received: 09.12.2021, Accepted: 16.04.2022

Class II and exhibits low solubility and high permeability.[11] It is a non-flavonoid polyphenolic compound.[12,13] The compound was first isolated from the root of *Reynoutria japonica* Hutt. (previously *Polygonum cuspidatum* Siebold & Zucc.) from Polygonaceae, a plant used in traditional Chinese and Japanese medicine.[14] RSV was studied for its different activities *viz.* anti-inflammatory, immunomodulatory, cardioprotective, antioxidant, anticancer, and for promoting vascular endothelial function.[15,16] It stimulates endothelial nitric oxide (NO) synthase activity and facilitates vascular endothelial growth factor (VEGF) expression,[17] thus providing vascular protection and improving the blood supply.[18]

Lakshmanan et al.[18] and co-workers reported RSV-loaded nanofibrous scaffolds accelerated the wound healing process by regenerating dermal tissue. In a study conducted by Poornima and Korrapati[19], composite nanofibrous scaffolds loaded with RSV and ferulic acid showed 100% wound closure within 15 days. RSV potentiates the activity of antioxidant enzymes superoxide dismutase and glutathione peroxidase and thus has a positive influence on wound healing.[20] RSV-loaded microparticles distributed in collagen laminin matrix scaffold showed improved wound healing without a serious inflammatory response.[21] Zhao et al.[22] and co-workers reported in their study that the direct local application of RSV in dorsal skin wound bed tissue activated AMP-activated protein kinase (AMPK) signaling pathway, resulting in rapid wound healing through effective vascularization.[22] Considering the beneficial effects of RSV in the wound healing process, the study was conducted to formulate RSV microsponges to promote wound healing.[9]

Moringa oleifera Lam. (Moringaceae) gum is natural gum obtained from the exudates of the plant. It is a hydrophilic plant polymer acting as an emulsifier, gelling agent, suspending agent, thickener, and stabilizer.[23] Being a natural gum, it is biocompatible, non-toxic, environmental friendly, and economical to cost and biodegradable in nature.[24] It has antimicrobial activities against various strains of bacteria.[25] Arabinogalactan, a polysaccharide present in the *M. oleifera* gum, has been reported to stimulate cell proliferation, which in turn promotes tissue reepithelialization and reorganization of the tissues at the wound site.[26,27]

The current scenario focuses on treating the wound at an economical cost with easy applicability and no pain to the patient. Most of the microorganisms are resistant toward the current synthetic drug and therefore a need arise to explore natural drugs with minimum dose and maximum effect. The synthetic gel formulations for wound healing cause burning sensation, produce rashes on the skin, and even damage the skin around the wound area. Effective wound healing requires that the active ingredients should be delivered in high concentration at the target site or the contact time of the active ingredient on the surface of the skin or within epidermis should be increased, thereby preventing its penetration inside the skin as well eliminating the skin aliments associated with the synthetic agents. To achieve this, porous microsponges loaded with active ingredients prove to be the best choice,[2] which can be incorporated into gels, creams, lotions, and powders. Microsponges also help modify the drug release rate, thus reducing the frequency of application of the dosage form and improving patient compliance. Controlling the rate of moisture at the wound site locally, through the application of gel is an important criterion required for faster wound healing.[4] Hence, this work was carried out with an aim to formulate RSV-loaded microsponges incorporated into the gel base of *M. oleifera* gum to make the drug available at the wound site.

The hypothesis of the research work is to achieve the dual advantage of sustained release of the drug due to its entrapment, in the porous structure of the microsponges as well as the benefits of *M. oleifera* gel base for efficient wound healing without any irritation and damage to the skin around the wound site.

MATERIALS AND METHODS

Materials

Herbo Nutra Chemical Supplier, New Delhi, India, supplied RSV. Evonik India Pvt. Ltd. Mumbai, India gifted Eudragit RL 100. *M. oleifera* gum were collected from a local market. Magnesium stearate, acetone, *n*-hexane, methyl paraben, propyl paraben, propylene glycol, and triethanolamine (TEA) were purchased from Loba Chemie, Mumbai, India.

Methods

Preparation of microsponges

Oil in oil emulsion solvent diffusion method was used for the preparation of microsponges.[28] The internal phase consisted of RSV, Eudragit RL 100, magnesium stearate (Loba Chemie, Mumbai, India), and acetone (Loba Chemie, Mumbai, India). Appropriate ratios of drug and polymer were dissolved in acetone, magnesium stearate (3% w/v of solvent) was added to it, which was then sonicated in ultrasonic bath 70 kHz frequency for 20 to 25 min (Bio-Techniques, Mumbai, India) to get a homogenous dispersion. Magnesium sterate in appropriate concentration acts as a droplet stabilizer in the formulation of microsponges, it reduces interfacial tension between light liquid paraffin and formed microparticles of Eudragit RL 100 and thus prevents flocculation resulting in the formation of stable discrete microsponges.[29] The obtained internal phase solution was then poured drop wise into cold liquid paraffin (external phase) and stirred at 800 rpm for 1 h using an overhead mechanical stirrer (EMTEK Instruments, Mumbai, India). Lastly, the solidified microsponges were filtered and washed with *n*-hexane to get the porous rigid structure, air dried at room temperature for 12 h and stored in desiccators for further study.[29,30]

Selection of formulation parameters

In the preliminary trials, the effect of formulation parameters; the ratio of drug: polymer (1:2, 1:3, and 1:4), the volume of acetone (5, 7.5 and 10 mL), the volume of light liquid paraffin (15 mL and 30 mL), volume of magnesium stearate (1.5, 3, and 5% w/v of internal phase solvent), and stirring speed (600 and 800 *rpm*) for a period of 90 min were evaluated on the formulation aspect of the microsponges.

Experimental design

Based on the preliminary results, it was found that the concentration of drug: polymer ratio (X1) and volume of internal phase solvent (X2) were the critical parameters governing the drug entrapment efficiency (Y1) and particle size (Y2). To further optimize these parameters, 3^2 full factorial design (Design Expert 11.0., Stat-Ease Inc., Minneapolis) was adopted to optimize the microsponge formulation (Table 1).

Determination of λ_{max} in ultraviolet (UV) spectroscopy

For the preparation of the stock solution (1000 µg/mL), 10 mg RSV was dissolved in 10 mL methanol. Stock solution (0.1 mL) was further diluted with methanol to get 10 µg/mL. The spectrum was scanned over the range of 200-400 nm. The standard calibration curve for RSV was then plotted at different drug concentrations (0.2-10 µg/mL) absorbance was measured using UV spectroscopy.

Characterization of microsponges

Production yield

Production yield was calculated using equation (1) and carried out in triplicate.[31]

$$Production\ yield = \frac{Practical\ mass\ of\ microsponges}{Therotical\ mass\ (polymer + drug)} \times 100 \quad (1)$$

Drug content and entrapment efficiency

RSV microsponges (10 mg) were dispersed in methanol (5 mL), followed by shaking for 10 min using vortex mixer and the final volume made of 10 mL using methanol. The resulted solution was filtered, diluted and the concentration of RSV was determined spectrophotometrically using a UV spectrophotometer (1800, Shimadzu, Japan) at λ_{max} 305.80 nm against a blank (methanol),[32] and tests were performed in triplicate using equations (2) and (3):

$$Drug\ content = \frac{Amount\ of\ drug\ in\ microsponges}{Amount of Microsponges} \times 100 \quad (2)$$

$$Drug\ entrapment\ efficiency = \frac{Actual\ drug\ content}{Theoretical\ drug\ content} \times 100 \quad (3)$$

Particle size

The particle size of RSV loaded microsponges was evaluated by optical microscope and repeated thrice to calculate the mean particle size. Approximately 50 microsponge particles were randomly measured. Edmondson's equation was used to estimate the average particle size of the microsponges:

$$Dmean = \sum \frac{nd}{n} \quad (4)$$

Where n: number of microsponges counted

D: Mean size range

In vitro drug release study

In vitro release studies of RSV-loaded microsponges were carried out in USP dissolution test apparatus (type II paddle) (Electrolab India PVT.LTD). An accurately weighed amount of RSV loaded microsponges (100 mg) were placed in the dissolution test apparatus containing 900 mL phosphate buffer pH 7.4 maintained at 37 ± 0.5°C. An aliquot (2 mL) of sample was withdrawn at definite time intervals for a predetermined time of 8 h. The samples were analyzed for the drug content spectrophotometrically at λ_{max} 305.80 nm. Each time after withdrawal of the sample, the aliquots were replaced with the same buffer solution pH to maintain sink condition.[30]

Scanning electron microscopy (SEM) and differential scanning calorimetric analysis of RSV microsponges

The morphology of the RSV microsponges was assessed by SEM (JEOL, JSM-6360-A, Tokyo, Japan)[33,34] and the thermal analysis was carried out using Differential Scanning Calorimeter (Mettler Star SW 12.10, Mumbai, India).[35]

Table 1. Formulation of microsponges using 3^2 factorial design

Formulation code	Drug: polymer (X_1)	Acetone volume (mL) (X_2)	Magnesium stearate (mg)	Actual drug content (%)	Production yield (%)	Entrapment efficiency (%) (Y_1)	Particle size (µm) (Y_2)
F1	3	7.5	225	35.12 ± 1.43	66.58 ± 1.41	72.71 ± 1.92	547 ± 1.50
F2	2	5	225	27.12 ± 1.43	56.11 ± 0.76	59.36 ± 1.35	564 ± 1.80
F3	2	10	150	23.31 ± 1.25	82.13 ± 1.38	88.27 ± 0.88	432 ± 1.77
F4	4	7.5	300	36.95 ± 0.96	74.55 ± 2.48	79.55 ± 1.29	581 ± 1.94
F5	3	10	300	34.32 ± 2.32	84.04 ± 1.72	87.93 ± 2.36	460 ± 2.47
F6	4	5	150	38.61 ± 1.75	62.93 ± 1.45	68.26 ± 1.34	586 ± 1.03
F7	2	7.5	300	25.09 ± 1.26	70.89 ± 1.2	75.2 ± 1.50	518 ± 2.55
F8	3	5	225	36.25 ± 1.34	60.42 ± 1.62	65.13 ± 1.11	576 ± 3.01
F9	4	10	150	36.05 ± 1.4	87.41 ± 1.17	91.75 ± 1.69	481 ± 0.90

Each value is the mean of three observations

Formulation of microsponge-loaded gel

M. oleifera gum (4%, w/w) was soaked in water for a period of 24 h, followed by drying at room temperature. The dried gum was washed with acetone to remove any impurities and then passed through sieve number 45. The purified powdered *M. oleifera* gum was soaked in water and the mixture was stirred at 600 rpm to obtain a uniform dispersion.[23] To the obtained homogenous dispersion, methyl paraben (1%), propyl paraben (0.05%), and propylene glycol (5%), were added. The pH of the *M. oleifera* gel base was adjusted by slow addition of triethanolamine, followed by the incorporation of RSV microsponges into the gel base. Microsponges equivalent to 4% (w/w) of RSV were added into the three batches of the gel base.

Characterization of microsponge-loaded gel

The gel formulations were characterized for their visual appearance, color, odor, and pH.[36]

Measurement of pH

The pH of the RSV microsponge gel was evaluated with a digital pH meter (Digital Instrument Corporation, Ahmedabad, Gujrat). The readings were recorded as the mean of three readings.[37]

Measurement of viscosity

Brookfield Viscometer (Brookfield Engineering Corporation, Ametek, Mumbai, India) was used to measure the viscosity of the RSV microsponge gel. The gel was placed in a beaker and viscosity was measured using spindle number 64 at 10 rpm after a period of three minutes. The readings were recorded as the mean of three readings.[38]

Texture profile analysis

A Texture Analyzer (CTX, Brookfield, Ametek, Mumbai, India) was used to conduct the texture profile analysis of RSV-loaded microsponge gel. The sample holder of a cone analytical probe (TA3/100) (30 mm diameter, 60°C) was completely filled with gel, followed by forcing the cone down into sample holder (1 mm/s and depth of 10 mm). Once, the trigger force of 5 g was achieved, the cone started to pierce the sample at a speed of 2 mm/s to a depth of 25 mm. After achieving the penetration up to a specified distance, the probe (cone) departed from the sample. The obtained force-time plot was used to determine the hardness and adhesiveness of the gel.[39]

Ex vivo diffusion study

The goat skin membrane was obtained from a local slaughter house and washed with water, scalpel was used to remove non-dermatome skin. Then, the skin membrane was soaked in phosphate buffer pH 7.4 for 24 h and then placed on the Franz diffusion cell (DBK diffusion cell, Peliyagoda, India). A predetermined amount of microsponges loaded gel (1 g) was placed on the donor side. The receptor medium was filled with phosphate buffer pH 7.4, maintained at 37 ± 0.5°C and continuously stirred at 300 rpm. To assess the amount of drug diffused, samples (2 mL) were collected from the receiver compartment at specific time intervals. An equal volume of fresh phosphate buffer pH 7.4 solution was used to replace the solution to maintain the sink condition. Collected samples were evaluated by UV spectrophotometer at λ_{max} 305.80 nm. The readings were recorded as the mean of three readings.[35,36,40,41]

In vivo studies

Healthy Albino Wistar rats of either sex weighing between 180 and 220 g were used for the study. The study protocol was approved by the Institutional Animal Ethics Committee (approval no: 1249/P0/Re/S/09/CPCSEA) and IAEC protocol number RSCPR/IAEC/2019/06. Animals were procured from the National Institute of Bioscience, Pune and house in the animal house of JSPM's Rajarshi Shahu College of Pharmacy and Research, Tathwade, Pune, maintained at 10-12 h light and dark cycle, provided with 23 ± 2°C temperature and 44-50% humidity with food and water *ad libitum* during the study.

Excision wound model

The rats were divided into four groups containing 6 rats each (n: 6). Group I sham-operated group, group II represents the placebo control group received *M. oleifera* gel base, group III is the treatment control group received RSV-loaded microsponge gel and group IV represents the standard control group received Megaheal gel-colloidal silver (ARISTO Pharmaceuticals Pvt. Ltd, Mumbai, India).

The dorsal furs of animals were removed using depilatory cream [Veet hair removal cream, Reckitt Benckiser (India) Ltd.] and anesthetized using pentobarbital sodium (40 mg/kg, *i.p.*, body weight). An impression was made and wound approximately 12 mm and 2 mm depth of full thickness was marked and created using forceps, surgical blade, and scissors.[42,43]

Treatments were started immediately after creating the wound on day 0 by daily application of above-mentioned gel formulations on the wounded area. Day 0 is considered as a wounding day, when the wound was created first. One g of each formulated gels and marketed gel mentioned above was applied once daily from day 0 until complete healing to the respective groups.

Measurements of wound contraction

The wounded area was monitored and measured using vernier caliper and the percentage contraction after every 4th day was calculated. The initial size of the wound was considered 100% using the following equation (4).[42]

$$\%\ Wound\ contraction = \frac{Initial\ wound\ area - Specific\ day\ wound\ area}{Initial\ wound\ area} \times 100 \quad (5)$$

Histology of wound granulating tissue

All the rats were anesthetized and specimen samples from the healed wound tissues were collected from each group and stored in 10% (v/v) formalin solution to conduct the histological examination.[44]

Statistical analysis

All results of wound closure were presented as mean ± standard deviation and analyzed using two-way analysis of variance (ANOVA) followed by Bonferroni *post hoc* test using Graph Pad Prism 5.0 to determine the statistical significance ($p \leq 0.001$) were considered as statistically significant.

RESULTS AND DISCUSSION

Preparation of microsponges

Oil in oil emulsion solvent diffusion method was used for formulating the microsponges. The results from the preliminary trial batches indicated the appropriate parameters required for the formulation of microsponges were the concentration of light liquid paraffin (30 mL), concentration of magnesium stearate (3%, w/v) and stirring speed of 800 rpm for a period of 90 min. The critical parameters affecting the drug entrapment efficiency (Y1) and the particle size (Y2) of the microsponges were identified as drug: polymer ratio (X1) and the volume of solvent (acetone) as an internal phase (X2), which were further optimized using the 3^2 full factorial design. An optimization technique was used to get desired concentration of drug: polymer ratio and volume of internal phase solvent to formulate microsponges with desired characteristics as shown in Table 1.

Determination of λ_{max} in UV

A solution of 10 µg/mL of RSV in methanol was scanned in the range of 200-400 nm. UV scan of the drug is shown below (Figure 1). The λ_{max} of the RSV was found to be 305.80 nm. The calibration curve for RSV was linear in the range of 2-10 µg/mL confirming the Beer-Lambert's law with the regression coefficient value (0.9994)

Drug entrapment efficiency

The drug entrapment efficiency of RSV-loaded microsponge formulations ranged from 59.36 ± 1.35% to 91.75 ± 1.69%.

Formulation F9 showed an entrapment efficiency of 91.75%. The ratio of polymer concentration and the volume of acetone in the formulation F9 was 1:4 and 10 mL, respectively. With the increase in the concentration of polymer, entrapment efficiency was increased due to more amount of polymer available to entrap the drug. Also, as the volume of the internal phase was increased, viscosity was decreased, resulting in uniform mixing of drug and polymer, forming a matrix that in turn enhanced the drug entrapment efficiency of the microsponges. As the concentration of polymer and the volume of the internal phase decreased, entrapment efficiency also decreased and was found to be 59.36%.

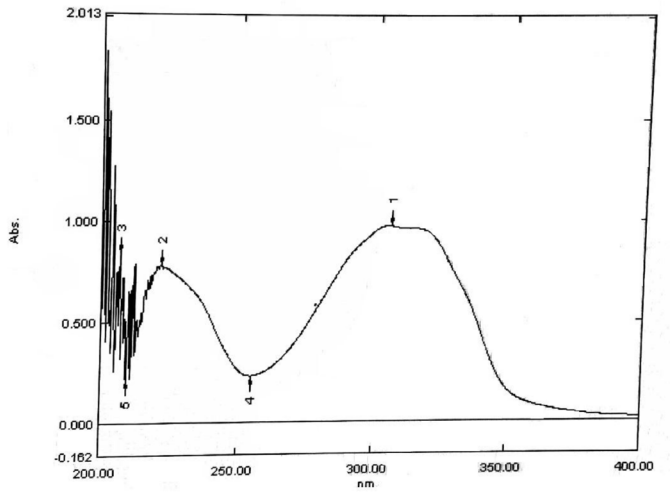

Figure 1. Ultraviolet spectrum of resveratrol

The statistical analysis by Design-Expert software (Design Expert 11.0., Stat-Ease Inc., Minneapolis) indicated the effect of factors influencing the entrapment efficiency. The effect of both independent variables (X1 and X2) on entrapment efficiency (Y1) was given by the following equation:

$$Y1 = 30.48944 + 2.80X1 + 5.00867X2 \quad (6)$$

A linear regression equation was obtained for the response of drug entrapment efficiency (Y1), which indicated a positive effect of X1 and X2 on the production of microsponges with a good fit R^2 value 0.979 and significant F value 103.63 and *p* value <0.0001.

From equation 5 and Figure 2a; the factor X1 showed a positive value, indicating a high drug entrapment efficiency in microsponges with the higher concentration of polymer. Also, with the increase in the polymer concentration, the diffusion rate of internal solvent from the microsponges decreased. This in turn led to the formation of a concentrated solution resulting in more time for droplet formation with increased precipitation of the drug in microsponges leading to increased entrapment efficiency.

A positive effect of X2 was observed on entrapment efficiency. The high volume of internal solvent was attributed to better solubilization of the drug in the internal solvent, resulting in enhanced entrapment efficiency of the microsponges.

Particle size

Polymer concentration and volume of the internal phase solvent are the major attributes determining the particle size of microsponges. The particle size of the microsponge formulation ranged from 432 to 586 µm.

The decrease in particle size could be attributed to the viscosity of the emulsion formed during processing. With the increase in the volume of the internal phase, the viscosity of emulsion decreased, resulting in reduction in globule size of emulsion droplets, leading to the formation of smaller particles and *vice versa*.[45]

The effect of (X1) and (X2) on the particle size of microsponges was explained by the following equation:

$$Y2 = +549.11 + 22.33X1 - 58.53X2 + 6.75X1X2 - 0.6667X_1^2 - 32.17X_2^2 \quad (7)$$

Equation (6) is a quadratic regression equation for the response Y2 with R^2 value 0.9899 and significant F value 59.08, *p* value <0.0034.

According to equation (6) and Figure 2; X1 showed a positive influence on particle size due to higher concentration of polymer, resulting in increased particle size due to more amount of the polymer available to entrap the drug. X2 exhibited negative influence on particle size indicating that, with the increase in the volume of internal phase, the viscosity of emulsion decreased, resulting in a reduction in globule size of emulsion droplets,

leading to the formation of smaller particles.

The interaction terms, *e.g.* X1 and X2, indicating the combined effect on the concentration of polymer and volume of internal solvent, have a positive effect on particle size. The reason for this could be an increase in the viscosity of the internal solvent. It was observed that with the increase in the concentration of polymer, the emulsion globules can hardly be subdivided into smaller particles.[32] The individual and the combined effects of the factors X1 and X2 on the response Y1 and Y2 responses are explained in the 3D surface graphs (Figure 2).

Optimization of microsponge formulation

The numerical optimization method was used to optimize the microsponge formulation. The desirability plot obtained indicates the optimum conditions needed for the formulation of microsponges with desired attributes. The optimized formulation (F5) showed minimal particle size (460 µm), higher drug entrapment efficiency (87.93 ± 2.369%) with desirability value of 0.915577.

SEM of RSV microsponges

SEM of the optimized batch of RSV microsponges (F5) showed uniform, spherical shape particle at 35X magnification, and a porous surface at 3000X magnification (Figure 3).

Differential scanning calorimetry

RSV exhibited a single sharp endothermic peak at 263˚C. RSV-loaded microsponges of batch F5 showed a broad endothermic peak at 215.90˚C and physical mixture of RSV and Eudragit RL 100 at 247˚C, respectively, Figure 4. RSV peak was not observed in RSV-loaded microsponge formulation due to encapsulation of the drug in matrix form of microsponges.[46] These results demonstrated no interaction between drug and polymer during the formation of microsponges.

In vitro drug release study of microsponges

In vitro drug release of formulations F4, F6, and F9 containing high polymer concentrations showed delayed release of drug (84.54%, 82.25%, and 79.05%, respectively within, 8 h). Due to the high amount of polymer, the escape of drug required more time to escape from the pores of the microsponge. Low concentrations of polymer in formulation F2, F3, and F7 resulted in rapid release of drug (96.87%, 94.59%, and 90.48% within 8 h) from microsponges. This fast drug release at the wound site was not satisfactory as sustained release of the drug is desirable for wound healing.[47] Formulation F1, F5, and F8 released 90.02%, 80.88%, and 86.82% drug within 8 h from the microsponges. Formulation F5 showed sustained

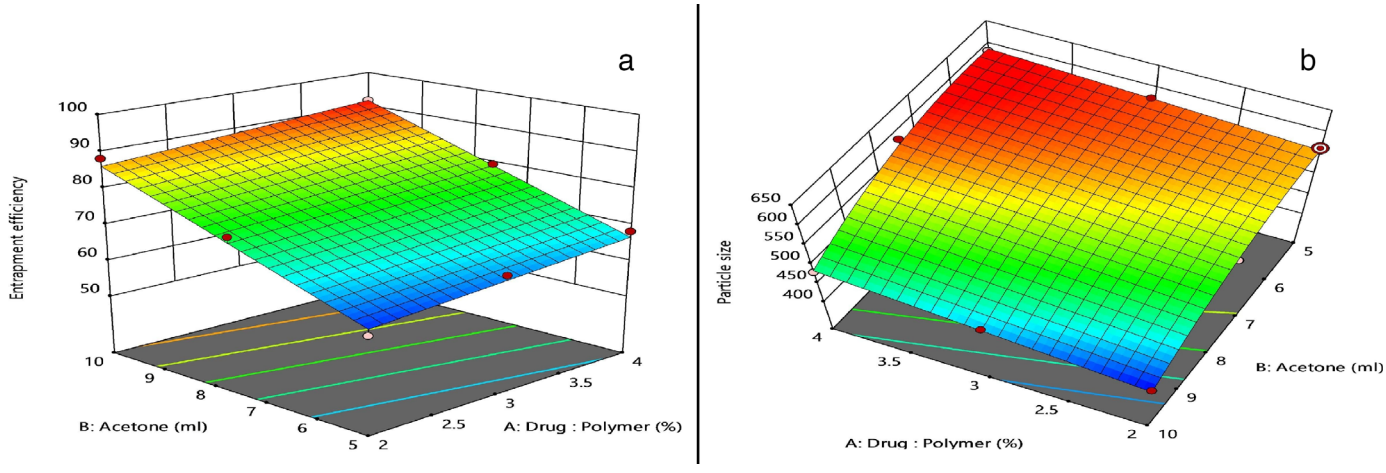

Figure 2. Three dimensional surface plots of (a) entrapment efficiency, (b) particle size

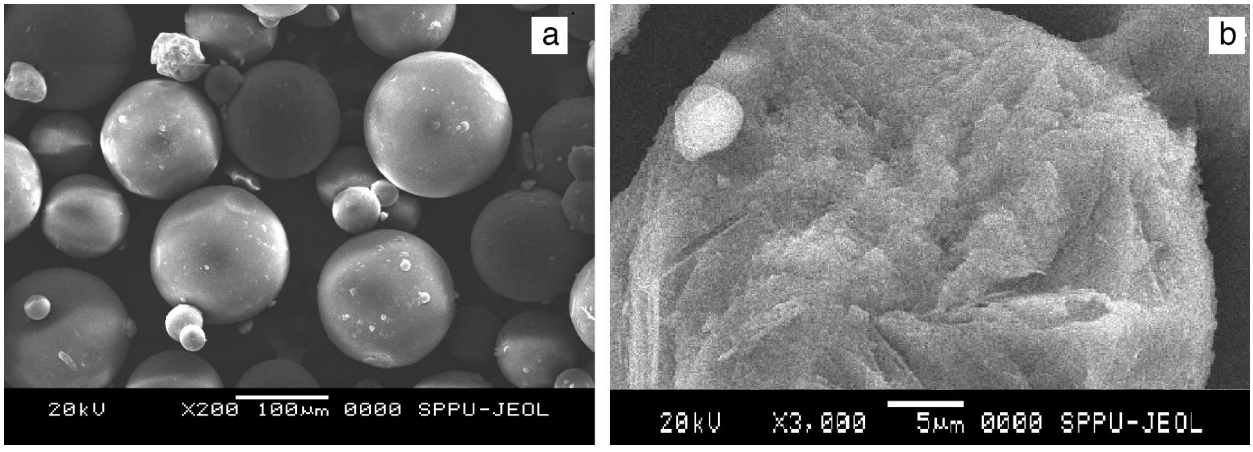

Figure 3. Scanning electron microscopy of resveratrol microsponges (a) 200x magnification, (b) 3000x magnification

drug release; thus, selected for further study in Figure 5. As the formulation F5 had a higher amount of drug: polymer ratio. The greater number of binding sites on the surface of Eudragit RL 100 was available due to the presence of ammonium groups leading to the stronger interaction of the drug with the polymer, which in turn prolonged the drug release.[48]

Evaluation of RSV microsponge-loaded M. oleifera gel

RSV microsponge-loaded *M. oleifera gel* was smooth, free from grainy particles with a pH close to 7.2 similar to wound pH,[49] indicating easy applicability of the gel to the wound site without any discomfort and irritation to the patient after application on wound area. The appropriate viscosity 15392 ± 5.567 exhibited by the gel indicated the easy of applicability and retention of gel at the wound site. Texture profile analysis of gel showed hardness (firmness) 273 g, adhesiveness 1.4 mJ, and adhesive force 79 g, Figure 6 indicating the easy spreadability of RSV-loaded microsponge gel. The *in vitro* drug diffusion studies of RSV microsponge-loaded *M. oleifera* gel showed 23.17% release in 3 h, 57.97% in 6 h and 68.98% in 8 h, respectively, thus indicating sustained release of RSV through the gel matrix of the polymer. The reason for this could be the swelling of the gel, which increased the diffusional path length, thereby sustaining the drug release.

In vivo study

Wound closure and contraction were assessed by image analysis visually (Figure 7). The wound area and % contraction after topical application of all gel formulations (*M. oleifera* gel base, RSV loaded microsponge gel, and standard gel) are presented in Table 2.

During treatment, the formulations were found to show its

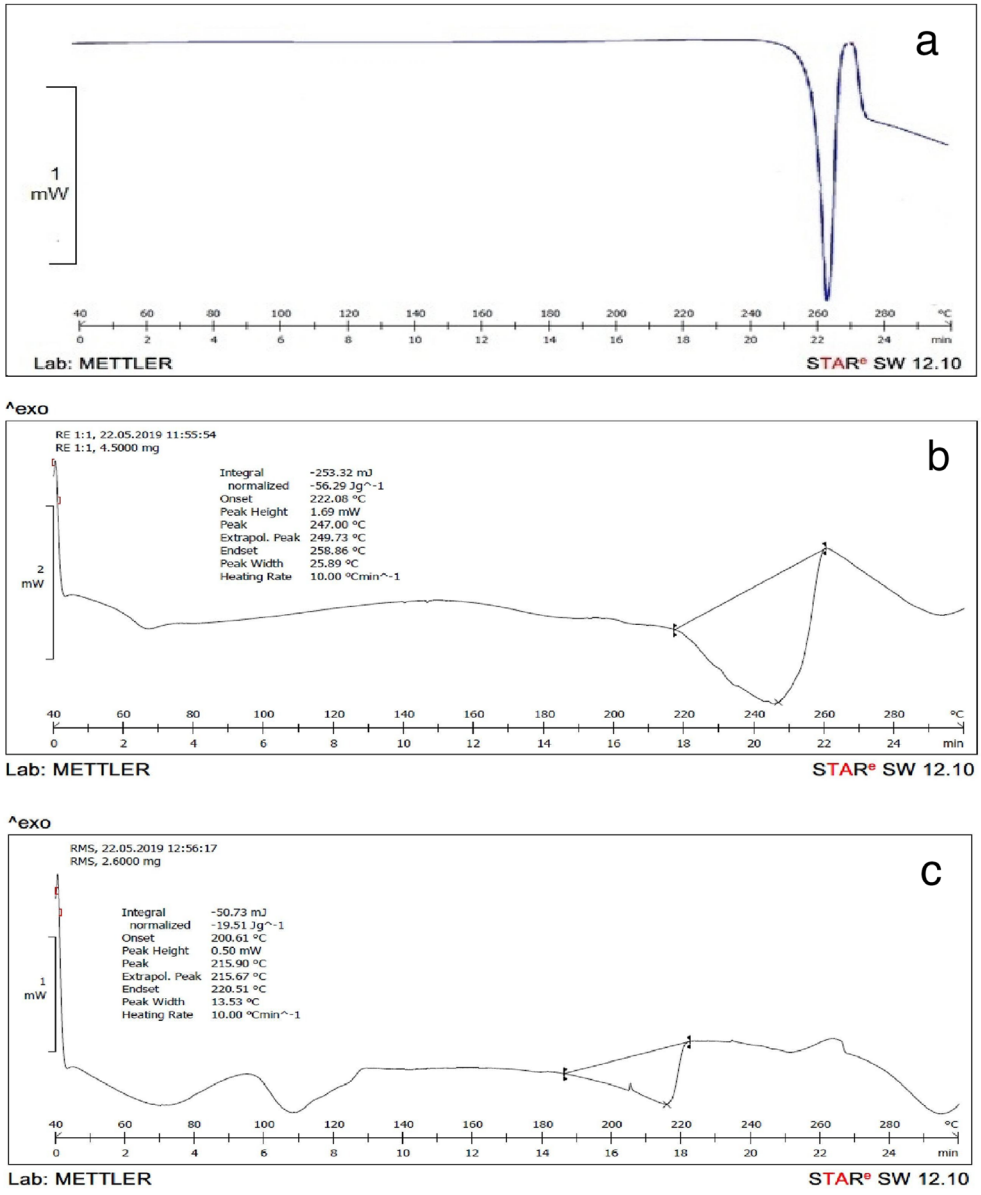

Figure 4. Differential scanning calorimetry thermograms of (a) resveratrol, (b) physical mixture, and (c) resveratrol loaded microsponges

preliminary effect from day 4 to day 16 (Figure 7). Group I (sham-operated) showed a slight wound healing even after 16 days of study. The percent wound closure of group I on days 0, 4, 8, 12, and 16 was 0%, 4.41%, 6.08%, 10.25%, and 17.66%, respectively. Group II referred as placebo-treated group received (*M. oleifera* gel base) exerted significant (p<0.001) increase in % wound closure on days 4, 8, 12, and 16 which was found to be 14.83%, 30.41%, 37.41%, and 45.83%, respectively, compared with sham-operated group. After a wound, the physiological reparative process of the body initiates, which involves movement of adjacent epithelial cells to the injured area. Arabinogalactan, a polysaccharide present in *M. oleifera*, is reported to influence this integrins recognition, thus influencing cell adhesion and affecting the healing process. The cell adhesion and the higher replication ability of the epithelial cells led to a faster stratification of the tissue and faster wound healing. Hence, on day 16, the percent wound closure in group II (*M. oleifera* gel base) was 45.83% compared to group I (sham-operated), which was 17.66% (p<0.001).

Gel containing RSV microsponges (group III) showed its maximum significant effect (p<0.001) by wound contraction with respect to the sham-operated group that proportionally confers the healing process and showed similar contraction as that of the standard control (group IV) on days 12 and 16. As *per* the rate of epithelization concerned, the RSV-loaded microsponge gel displayed its contributory role in accelerating epithelization (p<0.001) as compared to sham-operated group I and standard control group IV.

Many researchers have reported the role of polyphenolic compounds in promoting wound healing. The important events involved in the wound healing process are inflammation; cell proliferation and cell migration. Sirtuins (SIRTs) are NAD^+-dependent histone deacetylases which exhibit anti-inflammatory activity and stimulate cell proliferation and cell migration.[50] RSV acts as an activator of SIRTs, which act as one of the therapeutic strategies to enhance, wound healing. The activation of SIRTs by RSV suppresses the stimulation of TNF-α, which is an important cytokine causing inflammation and inactivates nuclear factor-κB, a transcription factor that is a major regulator of proinflammatory cytokine expression thus exhibiting anti-inflammatory effects.[51,52] The activation of SIRTs by RSV enhances the production of nitric oxide, which is involved in re-epithelialization, neovascularization, and collagen synthesis.[53] NO production also accelerates wound closure by recreation of keratinocyte proliferation.[54]

Group III showed significant (p<0.001) increase in percent wound closure at days 4, 8, 12, and 16, which was found to be 70.58%, 98.33%, 99.33%, and 99.41%, respectively, when compared with sham operated and standard control group. Reason for this could be the *M. oleifera* gel base, which provided suitable moist environment required for wound management. In the moist

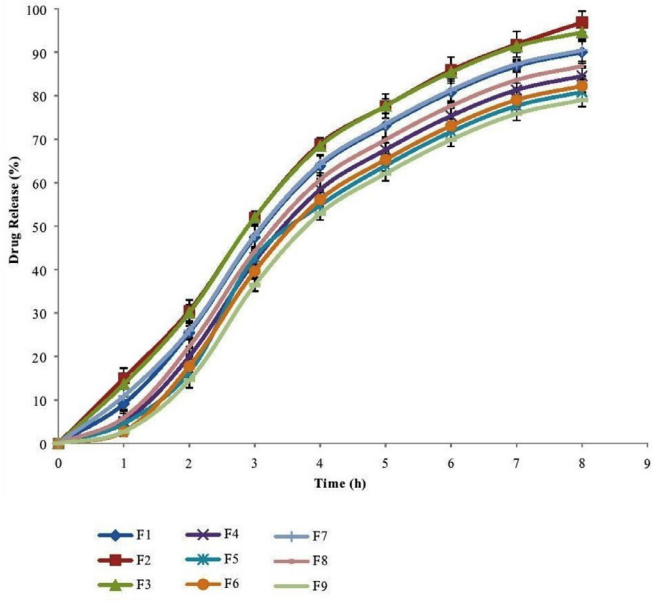

Figure 5. *In vitro* drug release of resveratrol-loaded microsponges

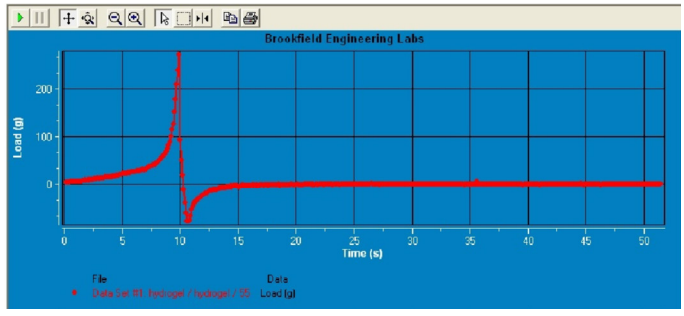

Figure 6. Spreadability of resveratrol-loaded microsponge gel

Table 2. Effect of resveratrol loaded microsponge gel on wound closure and % wound contraction in excision wound model

	Group I		Group II		Group III		Group IV	
	Area (cm)	% contraction	Area (cm)	% contraction	Area (cm)	% contraction	Area (cm)	% contraction
Day 0	1.200 ± 0.008	0	1.200 ± 0.007	0	1.200 ± 0.003	0	1.200 ± 0.008	0
Day 4	1.147 ± 0.032	4.41	1.022 ± 0.008***	14.83	0.353 ± 0.009***	70.58	0.194 ± 0.006***	83.83
Day 8	1.127 ± 0.040	6.08	0.835 ± 0.009***	30.41	0.020 ± 0.009***	98.33	0.008 ± 0.008***	99.33
Day 12	1.077 ± 0.061	10.25	0.751 ± 0.024***	37.41	0.008 ± 0.009***	99.33	0.007 ± 0.008***	99.41
Day 16	0.988 ± 0.015	17.66	0.650 ± 0.007***	45.83	0.007 ± 0.008***	99.41	0.008 ± 0.008***	99.33

All results of wound closure were presented as mean ± standard deviation. ***(p<0.001) to determine statistical significance

environment the epithelial cells migrate more readily compared to dry ones; also the growth factors are active, readily available, and synthesized in moist environments.[4] Arabinogalactan, a polysaccharide present in the *M. oleifera* gum, has been reported to stimulate cell proliferation, which in turn promotes tissue re-epithelialization and reorganization of the tissues at the wound site, thus, promoting faster wound healing.[26,27] The prolonged release of RSV through gel and further through microsponges formulated with Eudragit RL 100 indicated the retention of the drug in the porous structure of microsponges to slowly release it at the target site to heal wound. The mucoadhesive and the hydrophilic properties of Eudragit RL 100 permitted the retention of the RSV microsponges at the wound site, ensuring the availability of higher concentration of drug at the wound area of the skin as well as maintaining its ability to preserve the moisture required for wound healing. The solubility of RSV in phosphate buffer pH 7.4 might have also favored faster drug diffusion in wound area to achieve faster healing. Hence, the topical application of gel containing RSV microsponges in an excision wound model in rats successfully closed and healed the wound within day 8. It was observed that on day 4, drying of the wound was observed and the wound area was reduced to 0.353 ± 0.009 in group III. It was further observed that, on day 8, the wound was completely dried and the wound area was further reduced to 0.020 ± 0.009. In control sham group I, the area of the wound was 1.127 ± 0.040 even on day 8. In the present study, RSV-loaded microsponge gel showed prolonged drug release and retain on the skin to accelerate the wound healing process followed by wound contraction within 8-12 days, by reducing scar formation. Thus, fulfilling the hypothesis of the use of microsponge technology, where a higher concentration of entrapped RSV is available at the wound area of the skin with

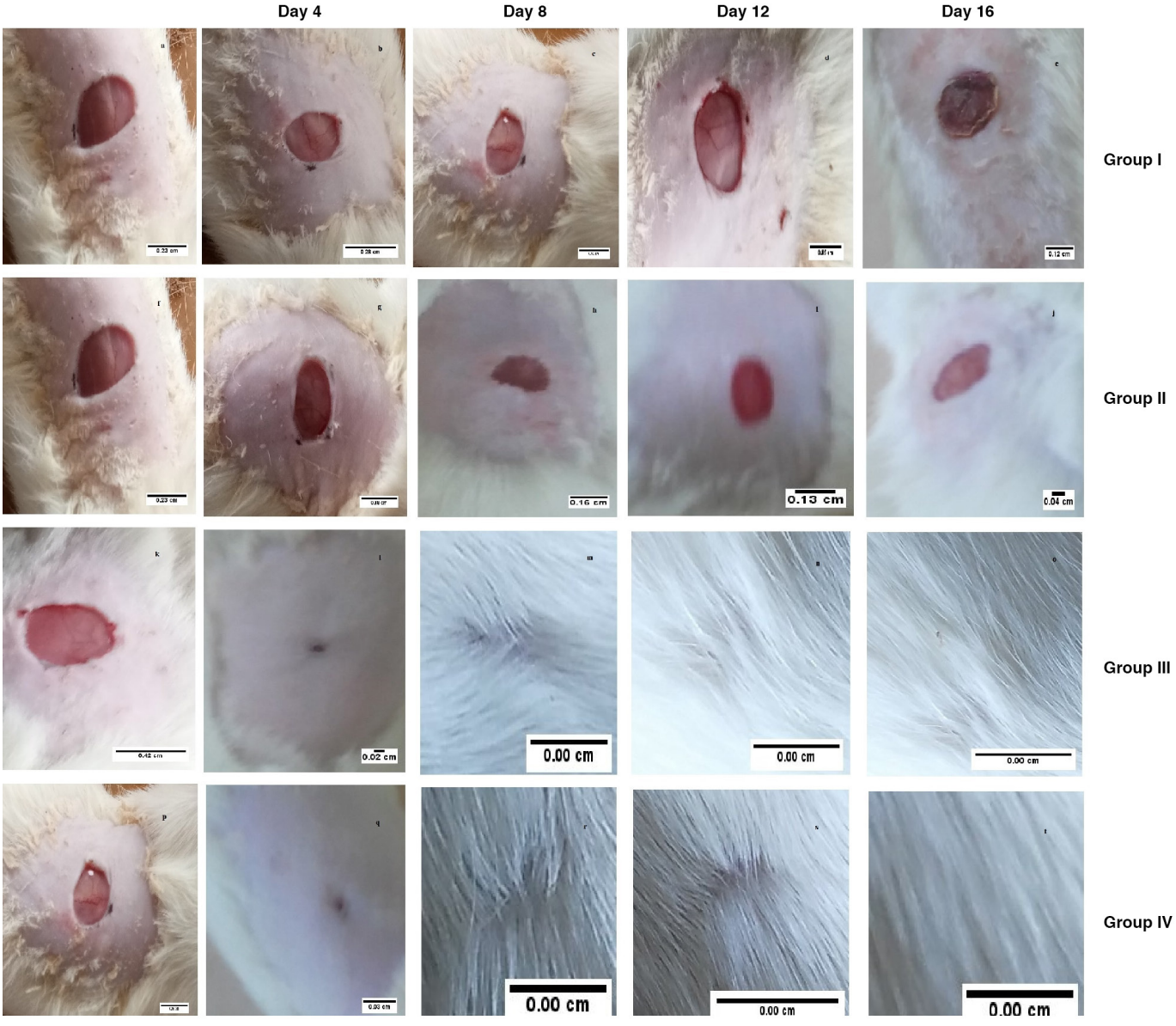

Figure 7. Photographs of wounds in rats in group I (sham-operated): (a) wound created on day 0, (b) wound on day 4, (c) wound on day 8, (d) wound on day 12 and (e) wound on day 16; group II (placebo): (f) wound created on day 0, (g) wound on day 4, (h) wound on day, (i) wound on day

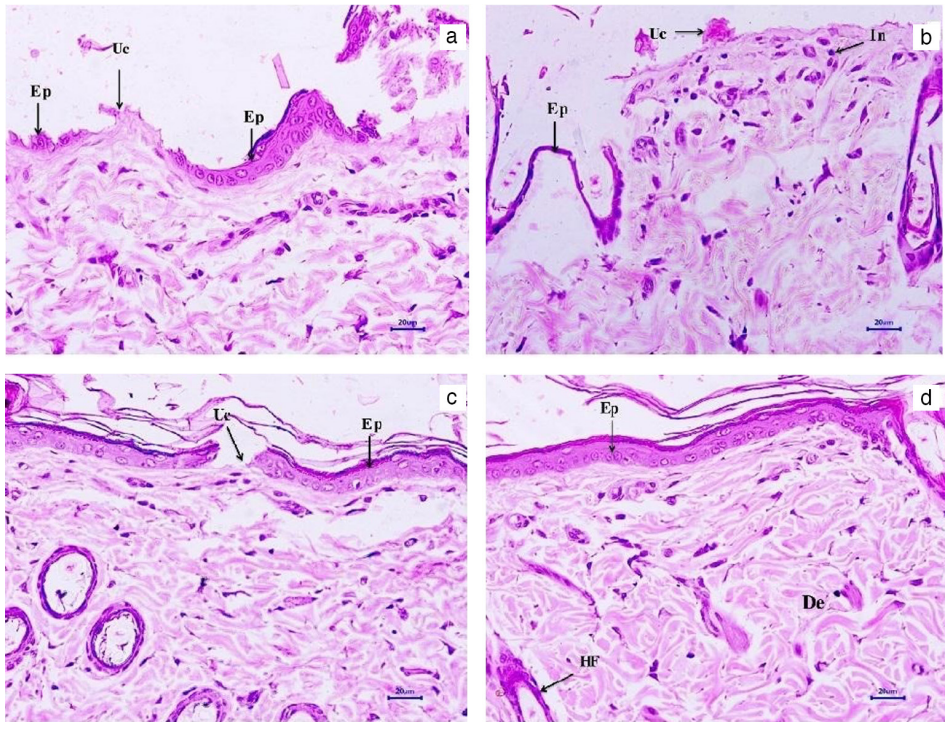

Figure 8. Histopathological sections of wound on day 16 of (a). Sham-operated, (b) placebo, (c) resveratrol-loaded microsponge gel, (d) standard gel

sustain release and the benefits of *M. oleifera* gel for efficient wound healing with no irritation and damage to the skin around the wound.

Histopathology

A histopathological study was conducted to observe any pathological changes in rat skin during application of formulated gels. The tissue samples of excision wounds were given for histopathological studies on day 16 (Figures 8a-d).

Platelet coagulation, cytokine and pro-inflammatory mediators, erythrocytes, blood vessels, fibroblast, mast cell, fibrin thread, ulceration, and development of newly formed epithelium in the sham-operated group (group I) was observed Figure 8b. In the placebo, treated skin (group II) showed slight ulceration and inflammation. Start of fibroplasia-collagen synthesis and deposition and arrival of neutrophils, macrophages, and slight formation of epithelial bridge with newly formed epithelium were observed Figure 8c. Group III showed a rapid reduction in ulceration with reduced inflammatory cells, fibroplasia-collagen synthesis, granulation tissue formation, matrix formation, and collagen fiber deposition, regenerated epithelium. The integrity of the basement membrane was preserved. Healing by a process of epithelization was observed in group III Figure 8c. In the standard group IV, Figure 8d reveals epithelization with angiogenesis, regeneration of the epidermis, dermis, hair follicles, and reduced inflammatory cells with no ulceration. Collagen fibrin cross linking and scar maturation was seen.

These results are in accordance with the previous studies, stating that RSV increases the synthesis of collagen fibers, increases granulation by enhancing angiogenesis, scar formation, and improvement in wound healing.[9,55,56]

CONCLUSION

In conclusion, RSV-loaded microsponge gel was successfully formulated and developed for wound healing. Microsponges were prepared by oil in oil emulsion solvent diffusion method using Eudragit RL 100. Microsponges-released drug in a sustained manner at the wound site through pores and *M. oleifera* gum gel provided a moist environment in the later stages of wound healing. This unique combination of RSV-loaded microsponges in *M. oleifera* gel demonstrated rapid wound healing and could be considered as easy to apply with no pain dosage form and a potential alternative to the current synthetic agents used for treating wound healing, thus improving the patient compliance and reducing the global burden of wound care.

Ethics

Ethics Committee Approval: The study protocol was approved by the Institutional Animal Ethics Committee (approval no: 1249/P0/Re/S/09/CPCSEA) and IAEC protocol number RSCPR/IAEC/2019/06.

Informed Consent: Not applicable.

Peer-review: Externally peer-reviewed.

Authorship Contributions

Surgical and Medical Practices: D.A., Concept: V.P., Design: V.P., Data Collection or Processing: V.P., Analysis or Interpretation: V.P., Literature Search: V.P., S.C., Writing: V.P., S.C.

Conflict of Interest: No conflict of interest was declared by the authors.

Financial Disclosure: The authors thank Herbo Nutra chemical suppliers, New Delhi, India for providing RSV and Evonik India PVT. LTD, Mumbai, India for providing gift sample of Eudragit RL 100.

REFERENCES

1. Kaity S, Maiti S, Ghosh AK, Pal D, Ghosh A, Banerjee S. Microsponges: a novel strategy for drug delivery system. J Adv Pharm Tech Res. 2010;1:283-290.
2. Nacht S, Kantz M. The microsponge: a novel topical programmable delivery system. Top Drug Deliv Syst. 1992;42:299-325.
3. Jain N, Sharma PK, Banik A. Recent advances on microsponge delivery system. Int J Pharm Sci Res. 2011;8:13-23.
4. Pandit AP, Patel SA, Bhanushali VP, Kulkarni VS, Kakad VD. Nebivolol-loaded microsponge gel for healing of diabetic wound. AAPS PharmSciTech. 2010;18:846-854.
5. Cho AR, Chun YG, Kim BK, Park DJ. Preparation of chitosan-TPP microspheres as resveratrol carriers. J Food Sci. 2014;79:568-576.
6. Pandima DM, Sekar M, Chamundeswari M. A novel wound dressing material-fibrin-chitosan-sodium alginate composite sheet. Bull Master Sci. 2012;35:1157-1163.
7. Momoh MA, Kenechukwu FC, Nnamani PO, Umetiti JC. Influence of magnesium stearate on the physicochemical and pharmacodynamic characteristics of insulin-loaded Eudragit entrapped mucoadhesive microspheres. Drug Deliv. 2015;22:837-848.
8. Kouchak M, Handali S, Naseri Boroujeni B. Evaluation of the mechanical properties and drug permeability of chitosan/Eudragit RL composite film. Osong Public Health Res Perspect. 2015;6:14-19.
9. Yaman I, Derici H, Kara C, Kamer E, Diniz G, Ortac R, Sayin O. Effects of resveratrol on incisional wound healing in rats. Surg Today. 2013;43:1433-1438.
10. Diegelmann RF, Evans MC. Wound healing: an overview of acute, fibrotic and delayed healing. Front Biosci. 2004;9:283-289.
11. Seljak KB, Berginc K, Trontelj J, Zvonar A, Kristl A, Gašperlin M. A self-microemulsifying drug delivery system to overcome intestinal resveratrol toxicity and presystemic metabolism. J Pharm Sci. 2014;103:3491-3500.
12. Ahmadi Z, Mohammadinejad R, Ashrafizadeh M. Drug delivey systems for resveratrol, a non-flavonoid polyphenol: emerging evidence in last decades. J Drug Deliv Sci Tec. 2019;51:591-604.
13. Burns J, Yokota T, Ashihara H, Lean ME, Crozier A. Plant foods and herbal sources of resveratrol. J Agric Food Chem. 2002;50:3337-3340.
14. Liu C, Tong P, Yang R, You Y, Liu H, Zhang T. Solidified phospholipid-TPGS as an effective oral delivery system for improving the bioavailability of resveratrol. J Drug Deliv Sci Tech. 2019;52:769-777.
15. Amri A, Chaumeil JC, Sfar S, Charrueau C. Administration of resveratrol: what formulation solutions to bioavailability limitations? J Control Release. 2012;158:182-193.
16. Das S, Das DK. Resveratrol: a therapeutic promise for cardiovascular diseases. Recent Pat Cardiovasc Drug Discov. 2007;2:133-138.
17. Penumathsa SV, Thirunavukkarasu M, Koneru S, Juhasz B, Zhan L, Pant R, Menon VP, Otani H, Maulik N. Statin and resveratrol in combination induces cardioprotection against myocardial infarction in hypercholesterolemic rat. J Mol Cell Cardiol. 2007;42:508-516.
18. Lakshmanan R, Campbell J, Ukani G, O'Reilly Beringhs A, Selvaraju V, Thirunavukkarasu M, Lu X, Palesty JA, Maulik N. Evaluation of dermal tissue regeneration using resveratrol loaded fibrous matrix in a preclinical mouse model of full-thickness ischemic wound. Int J Pharm. 2019; 558:177-186.
19. Poornima B, Korrapati PS. Fabrication of chitosan-polycaprolactone composite nanofibrous scaffold for simultaneous delivery of ferulic acid and resveratrol. Carbohydr Polym. 2017;157:1741-1749.
20. Sayin O, Micili SC, Goker A, Kamaci G, Ergur BU, Yilmaz O, Guner Akdogan G. The role of resveratrol on full - thickness uterine wound healing in rats. Taiwan J Obstet Gynecol. 2017;56:657-663.
21. Gokce EH, Tuncay Tanrıverdi S, Eroglu I, Tsapis N, Gokce G, Tekmen I, Fattal E, Ozer O. Wound healing effects of collagen-laminin dermal matrix impregnated with resveratrol loaded hyaluronic acid-DPPC microparticles in diabetic rats. Eur J Pharm Biopharm. 2017;119:17-27.
22. Zhao P, Sui BD, Liu N, Lv YJ, Zheng CX, Lu YB, Huang WT, Zhou CH, Chen J, Pang DL, Fei DD, Xuan K, Hu CH, Jin Y. Anti-aging pharmacology in cutaneous wound healing: effects of metformin, resveratrol, and rapamycin by local application. Aging Cell. 2017;16:1083-1093.
23. Panda D, Si S, Swain S, Kanungo SK, Gupta R. Preparation and evaluation of gels from gum of *Moringa olifera*. Indian J Pharm Sci. 2008;68:777-780.
24. Jarald EE, Sumati S, Edwin S, Ahmad S, Patni S, Daud A. Characterization of *Moringa oleifera* Lam. gum to establish it as a pharmaceutical excipient. Indian J Pharm Edu. 2011;46:211-216.
25. Onsare JG, Kaur H, Arora DS. Antimicrobial activity of *Moringa oleifera* from different locations against some human pathogens. AJPS. 2013;1:80-91.
26. Raja W, Bera K, Ray B. Polysaccharides from *Moringa oleifera* gum: structural elements, interaction with β-lactoglobulin and antioxidative activity. RSC Advances. 2016;79:75699-75706.
27. Burgalassi S, Nicosia N, Monti D, Falcone G, Boldrini E, Fabiani O, Lenzi C, Pirone A, Chetoni P. Arabinogalactan as active compound in the management of corneal wounds: *in vitro* toxicity and *in vivo* investigations on rabbits. Curr Eye Res. 2011;36:21-28.
28. Mahant S, Kumar S, Nanda S, Rao R. Microsponges for dermatological applications: perspectives and challenges. Asian J Pharm Sci. 2020;15:273-291.
29. Zaki Rizkalla CM, latif Aziz R, Soliman II. *In vitro* and *in vivo* evaluation of hydroxyzine hydrochloride microsponges for topical delivery. AAPS Pharm SciTech. 2011;12:989-1001.
30. Abdellatif AAH, Zayed GM, Kamel HH, Mohamed AG, Arafa WM, Khatib AM, Sayed OM. A novel controlled release microsponges containing Albendazole against *Haemonchus contortus* in experimentally infected goats. J Drug Deliv Sci Tec. 2017;43:469-476.
31. Pawar AP, Gholap AP, Kuchekar AB, Bothiraja C, Mali AJ. Formulation and evaluation of optimized oxybenzone microsponge gel for topical delivery. J Drug Deliv. 2015;2015:261068.
32. Srinivas P, Reddy J. Formulation and evaluation of isonazide loaded nanosponges for topical delivery. Pharm Nanotechnol. 2015;3:68-76.
33. Jelvehgari M, Montazam H. Evaluation of mechanical and rheological properties of metronidazole gel as local delivery system. Arch Pharm Res. 2011;34:931-940.
34. Kumar PM, Ghosh A. Development and evaluation of metronidazole loaded microsponge based gel for superficial surgical wound infections. J Drug Deliv Sci Tec. 2015;30:15-29.

35. Wavikar P, Vavia P. Nanolipidgel for enhanced skin deposition and improved antifungal activity. AAPS PharmSciTech. 2013;14:222-233.

36. Shirsand SB, Para MS, Nagemdrakumar D, Kanani KM, Keerthy D. Formulation and evaluation of ketoconazole niosomal gel drug delivery system. Int J Pharm Invest. 2012;2:201-207.

37. Aiyalu R, Govindarjan A, Ramasamy A. Formulation and evaluation of topical herbal gel for the treatment of arthritis in animal model. Braz J Pharm Sci. 2016;52:493-507.

38. Pandit AP, Pol VV, Kulkarni VS. Xyloglucan based in situ gel of lidocaine HCL for the treatment of peridontosis. J Pharm (Cairo). 2016;2016:3054321.

39. Patel N, Padia N, Vadgama N, Raval M, Sheth N. Formulation and evaluation of microsponge gel for topical delivery of fluconazole for fungal therapy. J Pharm Invest. 2016;46:221-238.

40. Mahaparale PR, Nikam SA, Chavan MS. Development and evaluation of terbinafine hydrochloride polymeric microsponges for topical drug delivery. Indian J Pharm Sci. 2018;80:1086-1092.

41. Dev SK, Choudhury PK, Srivastava R, Sharma M. Antimicrobial, anti-inflammatory and wound healing activity of polyherbal formulation. Biomed Pharmacother. 2019;111:555-567.

42. Kumar PM, Ghosh A. Development and evaluation of silver sulfadiazine loaded microsponge based gel for partial thickness (second degree) burn wounds. Eur J Pharm Sci. 2017;96:243-254.

43. Nagar HK, Srivastava AK, Srivastava R, Kurmi ML, Chandel HS, Ranawat MS. Pharmacological investigation of the wound healing activity of *Cestrum nocturnum* (L.) ointment in Wistar Albino rats. J Pharm (Cairo). 2016;2016:9249040

44. Guerrero DQ, Fessi H, Allemann E, Doelker E. Influence of stabilizing agents and preparative variables on the formation of poly(d,l-lactic acid) nanoparticles by an emulsification-diffusion technique. Int J Pharm.1996:143:133-141.

45. Isailovic BD, Kostic IT, Zvonar A, Dorcevic VB, Gasperlin M, Nedovic VA, Bugarski BM. Resveratrol-loaded liposomes produced by different techniques. Innov Food Sci Emerg. 2013;19:181-189.

46. Dai T, Tanaka M, Huang YY, Hamblin MR. Chitosan preparations for wounds and burns: antimicrobial and wound healing effects. Expert Rev Anti Infect Ther. 2011;9:857-879.

47. Singh G, Pai RS. Atazanavir-loaded Eudragit RL100 nanoparticles to improve oral bioavailability: optimization and *in vitro/in vivo* appraisal. Drug Deliv. 2014;23:532-539.

48. Li M, Han M, Sun Y, Hua Y, Chen G, Zhang L. Oligoarginine mediated collagen/chitosan gel composite for cutaneous wound healing. Int J Biol Macromo. 2018;122:1120-1127.

49. Sen CK, Khanna S, Gordillo G, Bagchi D, Bagchi M, Roy S. Oxygen, oxidants, and antioxidants in wound healing: an emerging paradigm. Ann N Y Acad Sci. 2002;957:239-249.

50. Aioi A. Sirtuins in wound healing. Trends in Immunotherapy. 2017;1:114-120.

51. Zhu X, Liu Q, Wang M, Liang M, Yang X, Xu X, Zou H, Qiu J. Activation of SIRT1 by resveratrol inhibits TNF-α induced inflammation in fibroblasts. PLoS One. 2011;6:e27081.

52. Napetschnig J, Wu H. Molecular basis of NF-κB signaling. Annu Rev Biophys. 2013;42:443-468.

53. Mattagajasingh I, Kim CS, Naqvi A, Yamamori T, Hoffman TA, Jung SB, DeRicco J, Kasuno K, Irani K. SIRT1 promotes endothelium-dependent vascular relaxation by activating endothelial nitric oxide synthase. Proc Natl Acad Sci. 2007;104:14855-14860.

54. Rizk M, Witte M, Barbul A. Nitric oxide and wound healing. World J Surg. 2004;28:301-306.

55. Paulo L, Ferreira S, Gallardo E, Queroz JA, Domingues F. Antimicrobial activity and effects of resveratrol on human pathogenic bacteria. World J Microb Biot. 2010;26:1533-1538.

56. Afshar M, Taheri Hassanzadeh MM, Zardast M, Moghaddam A. The anigiogenetic effect of resveratrol on dermal wound healing in balb/c mice. Mod Care J. 2017;14:e66118.